

# Equilibrium and dynamical properties of few particle systems in quantum dots and bilayers

A.V. Filinov<sup>\*1,2</sup>, P. Ludwig<sup>1</sup>, V. Golubnychi<sup>1</sup>, M. Bonitz<sup>1</sup>, and Yu.E. Lozovik<sup>2</sup>

<sup>1</sup> Fachbereich Physik, Universität Rostock Universitätsplatz 3, D-18051 Rostock, Germany

<sup>2</sup> Institute of Spectroscopy RAS, Moscow region, Troitsk, 142190, Russia

Received 24 February 2003, revised 2003, accepted 2003

Published online 2003

PACS 36.40.Ei, 64.70.Nd, 71.10.-w, 71.35.-y

The equilibrium and dynamical properties of classical and quantum bilayers with spatially separated electrons and holes are investigated by a normal mode analysis and path integral Monte-Carlo (PIMC). For the low-density limit, where the particles are classical, we present results for the eigenfrequencies, eigenmodes and analyze the dependence on the inter-dot distance. Using PIMC we obtain the phase diagram of mesoscopic e-h-bilayers in the full space of temperature, density and interdot distance. Five different phases are identified: exciton liquid, exciton cluster (mesoscopic crystal), decoupled electron and hole crystals (Coulomb crystal), Coulomb liquid, electron-hole plasma.

**1 Introduction** Low-dimensional electron-hole systems in semiconductor heterostructures and quantum dots are of increasing experimental and theoretical interest because there qualitatively new physical effects can take place. One of the interesting systems is a two-layer system where in each layer the carriers are additionally confined by some external potential. Such a system of coupled quantum dots can be populated by carriers of different charge, e.g. under the action of a laser field, which results in the formation of bound states of pairs of spatially separated electrons and holes.

In this paper we report on computer simulations of two symmetric 2D quantum dots (QD's), one containing electrons and the other the same number of holes. In particular, we are interested in the ground state properties of this system, excitation spectrum and in the interplay between Wigner crystallization in the layers and its coexistence with interwell (IW) excitons. In order to give a reliable answer to these questions, we perform path integral Monte Carlo simulations (PIMC) fully including quantum effects which are crucial for the behavior of excitons and their correlations.

**2 Mesoscopic bilayer** We consider a system of two 2D layers containing electrons and holes, respectively, interacting through the Coulomb potential which is described by the Hamiltonian

$$\begin{aligned}\hat{H} &= H_e + H_h - \sum_{i=1}^{N_e} \sum_{j=1}^{N_h} \frac{e_i e_j}{\epsilon \sqrt{|\mathbf{r}_i - \mathbf{r}_j|^2 + d^2}}, \\ \hat{H}_k &= \sum_{i=1}^{N_k} \left[ -\frac{\hbar^2}{2m_i} \nabla^2 + V_k(\mathbf{r}_i) + \sum_{i < j}^{N_k} \frac{e_i e_j}{\epsilon |\mathbf{r}_i - \mathbf{r}_j|} \right], \quad k = e, h,\end{aligned}\quad (1)$$

where  $m_i$  and  $e_i$  are the masses and charges of the particles. We consider symmetric bilayers (SEHB) with  $m_e = m_h = m$ , with the same harmonic confinement potential in the electron and hole layers,

\* Corresponding author: e-mail: afilinov@id.ru, Phone: +49 0381 498 69 57, Fax: +49 0381 498 69 52

$V_e = V_h = \frac{1}{2}m\omega_0^2 r^2$  (model of 2D vertically coupled quantum dots). In the following we use the effective Hartree energy  $Ha = e^2/\epsilon a_B$  as (atomic) unit of energy and the effective Bohr radius  $a_B = \hbar^2\epsilon/(m^*e^2)$  as unit of length. Temperature  $T$  is also given in atomic units.

**3 Phase diagramm of e-h bilayer** Previous theoretical and MC simulations of *macroscopic* electron-hole bilayers have shown that this system exhibits a series of structural phase changes. In the case of classical bilayers it was shown [1] that in a certain domain of coupling strengths  $\Gamma = \langle U \rangle / k_B T$  and layer separation  $d$ , the particles form stable bound dipole pairs (“classical excitons”). Changing  $\Gamma$  and  $d$ , these “dipoles” may form a gase-like, liquid or solid phase. On the other hand, at large  $d$ , electrons and holes behave as two nearly independent strongly coupled Coulomb systems.

In the extreme quantum limit ( $T = 0$ ), the ground state of a *macroscopic* SEHB has been investigated with diffusion Monte Carlo [2]. Yet this analysis was restricted to only three phases: the excitonic phase, the spin unpolarized two-component plasma and the triangular Wigner crystal. As in the classical system [1] it was found that the inter-layer correlations lead to a stabilization of the 2D Wigner crystal. In the classical system, with decreasing layer separation  $d/a$ , ( $a$  is the mean interparticle distance), the classical coupling parameter  $\Gamma$  decreases and reaches a minimum value  $\Gamma_m \approx 100$  at  $d/a = 1.5$  (this value is slightly lower than the phase boundary  $\Gamma \approx 137$  separating a *Coulomb fluid* and *Coulomb solid* in a 2D one-component system). This stabilization effect is caused by changes in the interaction potential from Coulomb-like, at large  $d$ , to dipole-like at small layer separations. In the quantum case (at  $T = 0$ ) these changes in the coupling between neighboring particle pairs were also found to lead to an extension of the crystal phase to higher densities: from  $r_s \approx 37$  (independent layers,  $d \rightarrow \infty$ ) to  $r_s \approx 20$  for  $d/a \geq 1.5$  [2].

In the present paper we extend these previous investigations to *mesoscopic* electron-hole systems which have been found to exhibit much richer properties [7, 4, 5]. Similarly as in a single electron quantum dot [7], we expect that our results, first, will qualitatively be close to those for macroscopic systems, but that there may be some quantitative differences depending on the exact number of particles. Second, new phases are expected to emerge, such as relative orientational disordering of individual cluster shells [7]. Finally, our analysis extends to *finite* temperature and the whole density range, thus our results for the phase boundary should connect both limits discussed above: 1) classical case,  $T \neq 0$ ,  $a/a_B \rightarrow \infty$ , and 2) quantum case at  $T = 0$ .

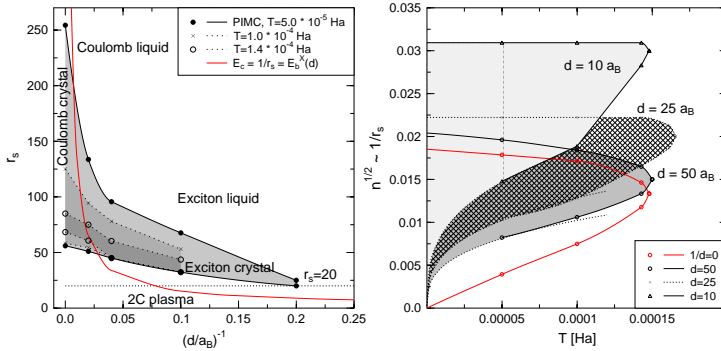


**Fig. 1** Phase diagram of the symmetric mesoscopic electron-hole bilayer with  $N_e = N_h = 16$ . The filled areas show the boundaries of the exciton WC at several values of temperature and  $d$ .

relative interparticle distance fluctuations, as these quantities have been found to be very sensitive to structural transitions (see [7] for details): a) with the formation of the mesoscopic crystal, fluctuations reach a minimum, while at the boundary of the solid-liquid transition fluctuations rapidly increase; b) from the

We have performed PIMC simulations for systems with  $N_e = N_h = 3, 8$  and  $16$  and several values of the interdot distance  $d = 50, 25, 10, 5 a_B$ , including the limiting case  $1/d \rightarrow 0$  that corresponds to the single-layer system. The effective densities of electrons and holes are controlled by the strength of the confinement,  $\omega_0$ . The temperature was varied in the range  $5 \times 10^{-5} \leq T \leq 2 \times 10^{-4}$ . The resulting phase diagram is shown in Fig. 1 (the shown result is for  $N_e = N_h = 16$  particles, for other  $N$  the results differ only quantitatively).

We identify different phases from an analysis of the intra- and inter-layer

behavior of the inter-layer fluctuations one can conclude when the electron and hole layers are coupled or decoupled (in the last case during exciton break up, the inter-layer distance fluctuations rapidly increase).

The left part of Fig. 1 shows that with decreasing  $d$  the exciton crystal phase shifts towards higher densities and shrinks. Eventually, the crystal phase vanishes for inter-layer separations  $d \lesssim 5a_B$ . As an additional result, we observe that the phase boundary also shrinks with increasing temperature. The shadowed areas are the regions where we found the bilayer solid at three different temperature values. These areas shrink with the increase of temperature. In this figure, the solid curve without symbols, is given by  $E_c = E_b^X(d)$ , along it the characteristic correlation energy due to Coulomb interaction inside layers becomes equal to the binding energy of vertical excitons. This line divides the phase plane into two regions where electrons and holes are bound in pairs or unbound. Due to this fact at least five different phases are possible. Above this line we found two phases: i) *exciton liquid*, ii) *exciton solid*. Below the line three phases can exist: iii) *Coulomb liquid*, iv) *Coulomb crystal*, v) *electron-hole plasma*. By Coulomb crystal we mean decoupled crystals of electrons and holes, when bond-orientational and translational order between two QD's is lost.

In the right part of Fig. 1 we show more in detail how the WC phase boundary depends on temperature,  $T$ , and  $d$ . The highest melting temperature is observed for intermediate layer distance,  $d \sim 25a_B$ . Interlayer attraction between electrons and holes leads to stabilization of the crystal phase: e.g., for the exciton cluster with  $N_e = N_h = 8$ , the coupling parameter,  $r_s = a/a_B$ , changes from  $r_s \approx 56$  (for  $d \rightarrow \infty$ ) to  $r_s \approx 20$  at  $d = 5a_B$ . For temperatures  $T \leq 5 \times 10^{-5}$  and density  $n^{1/2} \leq 0.015$  ( $r_s \gtrsim 67$ ), the phase boundary is well approximated by some critical value of the classical dipole coupling parameter  $\Gamma_D = e^2 d^2 / (a^3 k_B T) \sim (d/a_B)^{4/5}$ , as shown by the dotted lines starting at the origin.

**4 Energy spectrum of e-h bilayer** V.A.Schweigert, F.M.Peeters and A.Melzer [6, 8, 9] have performed investigations of spectral properties of single and double-layer electron clusters. In this section we extend these results to electron-hole bilayers.

An analysis of the ground state configurations of exciton clusters revealed that the mean interparticle distance in each layer,  $a(d)$ , has a strong dependence on the layer separation  $d$ , and shows two important limits: (I)  $d/a(d) \ll 1$ ,  $a(d)$  is determined only by dipole-dipole interaction and goes to zero with decreasing  $d$ ; (II)  $d/a(d) \gg 1$ , intra-layer Coulomb interaction dominates and the system behaves like two independent single layers. This causes the eigenfrequencies to become two-fold degenerate for *in-phase* and *anti-phase* motion of electrons and holes in both layers (see Fig. 2). In this case our results come into agreement with those for a single layer [8, 9]. In the limits (I) and (II),  $a(d)$  has different power law dependencies on the particle mass,  $m$ , charge,  $e$ , and trap frequency,  $\omega_0$ :  $a_I(d) = \left( \frac{e^2 d^2}{m \omega_0^2} A(N) \right)^{1/5}$ ,  
 $a_{II}(d) = \left( \frac{e^2}{m \omega_0^2} B(N) \right)^{1/3}$ , where  $A(N)$  and  $B(N)$  are constants of the order one, depending on the number of particles  $N$ .

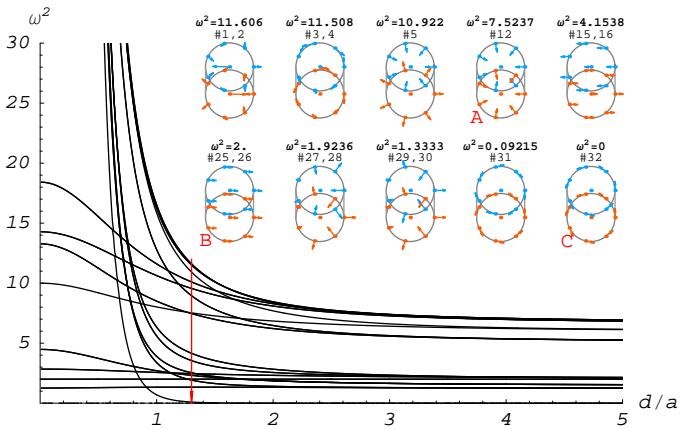


**Fig. 2** Excitation spectrum of normal modes for eight excitons as a function of distance  $d$ . The eigenfrequencies,  $\omega$ , are in units of the trap frequency  $\omega_0/\sqrt{2}$ . There are always  $2N$  normal modes ( $N$  is total particle number). Insets display the eigenvectors and eigenvalues for  $d/a = 1.3$  (along the vertical arrow in descending order).

The eigenvectors and eigenvalues for the ground state configuration of coupled electron-hole QD's were computed from the Hesse-Matrix:  $H_{ij} = \partial^2 H / \partial r_i \partial r_j$ , ( $\vec{r} = \{x_1, y_1, \dots, x_N, y_N\}$  is a vector of all particle coordinates) for many values of  $d$ . The results are represented in Fig. 2. The insets display the eigenvectors and eigenvalues at  $d/a = 1.3$ . One can notice that there are always  $2N$  orthogonal normal modes, most of which are two-fold degenerate, so in Fig. 2 we show only a selection of modes (by energy, in descending order). The eigenfrequencies,  $\omega$ , are given in units of  $\omega_0/\sqrt{2}$ .

For arbitrary particle number  $N$  one can always find three trivial modes: A) *rotation of the whole system*,  $\omega^2 = 0$ ; B) *vibration of the center of mass*,  $\omega^2 = 2$  (two-fold degenerate); C) *breathing mode*, i.e. coherent radial motion (compression/expansion) of all particles. Interestingly, we found that for C) an exact analytical result can be obtained for a large class of interactions of the form  $U(r) \sim \frac{e^2}{r^{1+p}}$  which includes (but is not limited to), the cases of Coulomb dipole and quadrupole interaction:

$$\omega_{br}^2 = 2m(3+p) = \begin{cases} 6, & p=0 \text{ Coulomb} \\ 10, & p=2 \text{ dipole} \\ 14, & p=4 \text{ quadrupole,} \end{cases}$$

where  $m = m_i/m_e$  ( $m$  is the mass of particle  $i$  in units of the electron mass  $m_e$ ). E.g., in a classical system of excitons interacting through a dipole potential, one observes for the breathing mode,  $\omega_{br}^2 = 20$ , for a symmetric electron-hole bilayer ( $m_i/m_e = (m_e + m_h)/m_e = 2$ ).

The analysis of the energy spectrum and normal modes as a function of  $d$  is crucial to understand the melting scenario in bilayer systems: I)  $d/a > 1$ , anti-phase rotation of shells in the electron and hole QD's has the lowest energy (mode 31, Fig. 2). With increasing temperature/density the QD's become decoupled and excitons are destroyed. This corresponds to the transition: *exciton crystal*  $\Rightarrow$  *Coulomb crystal*; II)  $d/a < 1$ , the lowest excitation energies are related to pairwise coupled motion of electrons and holes. As a result crystal melting proceeds via transition: *exciton crystal*  $\Rightarrow$  *exciton liquid* (excitons are preserved).

**5 Conclusion** To summarize, by performing extensive path integral Monte Carlo calculations and a normal mode spectrum analysis, we found that the interplay of inter-layer and intra-layer correlations determines the phase diagram of a system of inter-well excitons which contains (at least) five different phases. The phase diagram (in T, n, d-space) and the classical energy spectrum of mesoscopic e-h systems have been presented. The exciton crystal cannot exist in layers with  $d \lesssim 5a_B$  which generalizes the known result that excitons in a single layer cannot crystallize. Increase of density leads to exciton break-up and to the transition to an electron-hole "liquid".

Our work was limited to densities corresponding to  $r_s \gtrsim 20$ . At higher densities we expect an increasing role of exchange effects and appearance of a non-zero superfluid fraction of vertical excitons. Finally, while the observed phase diagram does not contain any approximations, the mode spectra, so far, can be obtained only for classical systems. To overcome these limitations is subject of ongoing work.

**Acknowledgements** This work has been supported by the Deutsche Forschungsgemeinschaft (BO-1366/3) and by grants for CPU time at the NIC Jülich and the Rostock Linux-Cluster "Fermion".

## References

- [1] An analysis of classical macroscopic e-h bilayers is performed in: P. Hartmann, Z. Donko, and G. Kalman, submitted to Phys. Rev. Lett.
- [2] Quantum macroscopic e-h bilayers has been investigated in: S. De Palo, F. Rapisarda, and G. Senatore, Phys. Rev. Lett. **88**, 206401 (2002)
- [3] A. Filinov, M. Bonitz and Yu.E. Lozovik, Phys. Rev. Lett. **86**, 3851 (2001)
- [4] E. Anisimovas and F.M. Peeters, Phys. Rev. B **66**, 075311 (2002)
- [5] M. Bonitz, V. Golubnychij, A.V. Filinov, Yu.E. Lozovik, Microelectronic Engineering **63**, 141 (2002)
- [6] G. Goldoni and F.M. Peeters, Phys. Rev. B **53**, 4591 (1996); I.V. Schweigert, V.A. Schweigert, and F.M. Peeters, Phys. Rev. Lett. **82**, 5293 (1999)
- [7] V.A. Schweigert and F.M. Peeters, Phys. Rev. B **51**, 7700 (1995)
- [8] A. Melzer, Phys. Rev. E **67**, 016411 (2003)